Experimental and Simulation Study Results of a Planetary Landing Site Selection System

ROGER T. SCHAPPELL* AND GAIL R. JOHNSON†
Martin Marietta Aerospace, Denver, Colo.

Introduction

TRADITIONALLY, the lack of knowledge regarding the details of planetary surfaces has dictated that proposed landings of unmanned spacecraft be made in relatively benign areas. The benefits of real-time selection of a smooth landing site were shown by the Apollo missions, where man performed the surface sensing and steering functions. For unmanned missions, an autonomous real-time surface sensing system is desirable to enable targeting geologically interesting landing sites on distant planets. The feasibility of such a system has been studied and the results reported here.

The Viking Mars mission was used in this study to arrive at a consistent and realistic set of design requirements and goals. The system must be compatible with the Viking lander in terms of mission profile, vehicle dynamics, interfacing, and environmental requirements. It also must be able to detect and avoid 22 cm obstacles during the latter portion of the terminal descent phase. Therefore a TV imaging system with contrast avoidance logic was chosen for the reference configuration.

System Operation

System operation is shown in Fig. 1. The Planetary Landing Site Selection System (PLS^3) is activated shortly after parachute release (approx 1200-m altitude). The predicted impact point (PIP), as determined by the lander computer, is provided to the PLS^3 to electronically position the 12° × 12° beam. The PIP is always within the 60° × 60° electronic gimbal authority (EGA). The 60° EGA is necessary to permit observing the PIP in spite of anticipated vehicle attitude excursions during the terminal landing phase. Use of electronic beam positioning obviates the need for extensive data processing of the entire area, mechanical gimbals, and reorienting the vehicle to observe the area about the PIP. The fixed 12° field of view encompasses the area consistent with the lander maneuver capability, and diminishes as a function of altitude while resolution improves. After the PLS^3 scans the surface, the video data are processed and a new impact point is selected (the area with the least contrast). A bias steering command to the lander computer enables maneuvering to the preferred landing site. The sequence is repeated at 1 sec intervals down to approximately 33 m from the surface.

Received August 11, 1972; presented as Paper 72-868 at the AIAA Guidance and Control Conference, Stanford, Calif., August 14–16, 1972; revision received October 24, 1972.

* Senior Staff Engineer.

† Aerospace Engineer.

Index categories: Unmanned Lunar and Interplanetary Systems; Entry Vehicles and Landers; Spacecraft Navigation, Guidance, and Flight-Path Control Systems.

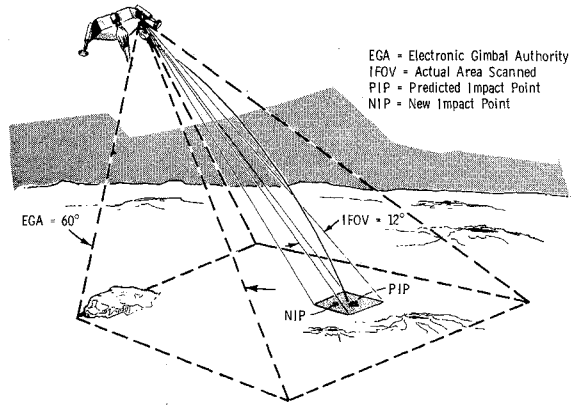

Fig. 1 System operation.

Operating time varies from 30 to 40 sec as a function of wind velocity and atmospheric density.

PLS^3 Reference Configuration

The PLS^3 configuration (Fig. 2) consists of an image dissector camera, area discrimination logic, and a simple raster scan mechanization. The optics, tube parameters, and scan control regulate beamwidth, resolution, and scan speed. The video signal is amplified, filtered, and sampled for a matrix of overlapping areas, which generates a figure of merit for each subset of areas. The coordinates for the area with the lowest figure of merit are then provided to the lander computer in the form of a bias command, which is actually the coordinates of the new impact point.

Data Processing

The fullband video signal from the image dissector is passed through a frequency-limiting filter to separate the surface feature characteristics. The reflectance from the various features (craters, slopes, ridges, breaks, boulders, rocks, etc.) indicated that each frequency band provided a measure of a peculiar set of surface characteristics.

To illustrate the simplified data processing scheme, a line scan and the filtered analog outputs for the lunar surface are shown in Fig. 3. Each of the three channels has significant data and represents the size, extent, and reflectance characteristics of the objects. After passing through a threshold detector, as illustrated for the midfrequency band, a varying pulse width is generated as a function of contrast. The signal is then modulated, counted, and weighted, which generates a figure of merit for the surface scanned.

Scan Layout

A fixed 12° × 12° scan is centered on the PIP with the surface area varying as a function of slant range (Fig. 4). A figure of merit is computed and stored for each Aij area. Each Aij area is defined by the four smaller squares surrounding its center point. These areas are then compared and the lowest Aij value

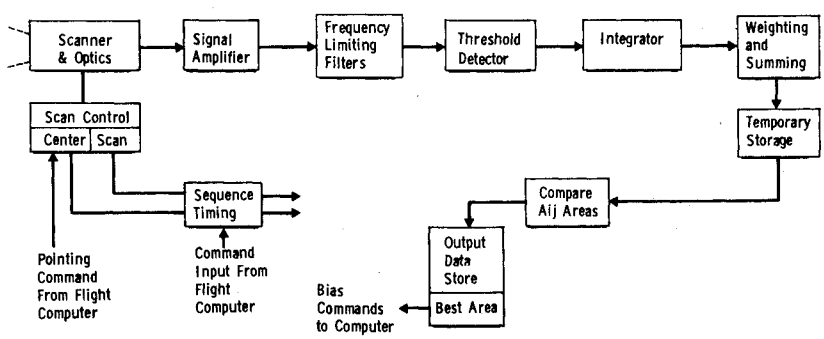

Fig. 2 PLS^3 configuration.

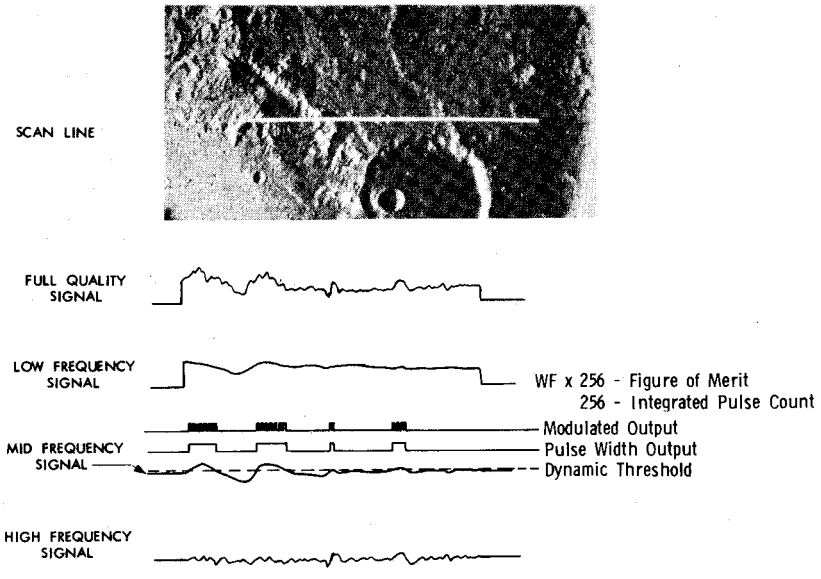

Fig. 3 Signal separation.

is selected as the NIP (the area of least contrast). The center point, PIP, and the arrows illustrate the nine possible steering coordinates.

The TV camera, scan electronics, and processing electronics operate together in a simple, straightforward mechanization. This same mechanization was simulated in the Viking six-degree-of-freedom (MOD6MV) simulation program and was breadboarded in the laboratory.

Digital Computer Simulation

The digital simulation models that functionally describe sensor operation and the additional flight computer software for the PLS[3] system were added, along with a surface model designed with the capability to generate and display a random distribution of different size obstacles containing: 1) fixed surface features for simulation run; 2) surface area containing all possible landing sites; 3) quasi-three-dimensional surface; and 4) access to surface features of any subregion.

The surface characteristic (Z) at any point is defined by

$$Z: [Z\varepsilon(0, 1, \ldots 7)\Lambda Z = f(x, y)\,\varepsilon x, y\varepsilon(1, 2, \ldots 500)]$$

where the function $f(x,y)$ is defined during initialization by a random number generator and the input cumulative probability for density of different size obstacles. A two-dimensional 500 × 500 grid was constructed, where an octal integer from zero to seven is assigned to each ordered pair of the array representing the size of the obstacle located at that coordinate of the generated surface. A zero was programed to represent a smooth flat surface; each increase up to seven was programed to represent a step to a larger rock, boulder, or obstacle. This limits the evaluation to eight levels of resolution but allows a considerable saving in machine core storage. The CDC 6500 computer word contains 60 binary bits, which means that by bit packing one computer word can represent 20 surface coordinates. By scaling the distance between the grid points, a landing surface of variable dimensions with eight levels of detail was mechanized that required 12,500 computer words to describe 250,000 surface coordinates. Access was designed into the system by defining a transformation that locates the surface generated (i.e., the ith row and jth column of the array) in planet-centered inertial space.

The grid point representing the PIP is determined by the location of a defined reference point, the input distance between adjacent grid points, and the vector from the reference point to the PIP. Once the coordinate of the PIP is known, the surface features of the area can be examined by interrogating the octal integers associated with surrounding grid points. The surface is visually displayed by using the CDC 280 software package to plot the nonzero grid points with the appropriate scale, and by plotting different size points that are relative to the size of the obstacle represented. Figure 5 represents a surface generated with a background of randomly distributed obstacles of varying size, and a 35-ft-radius crater that was artificially implanted by producing high densities of rocks and boulders in the appropriate areas. The plot of the PIP was superimposed on the displayed

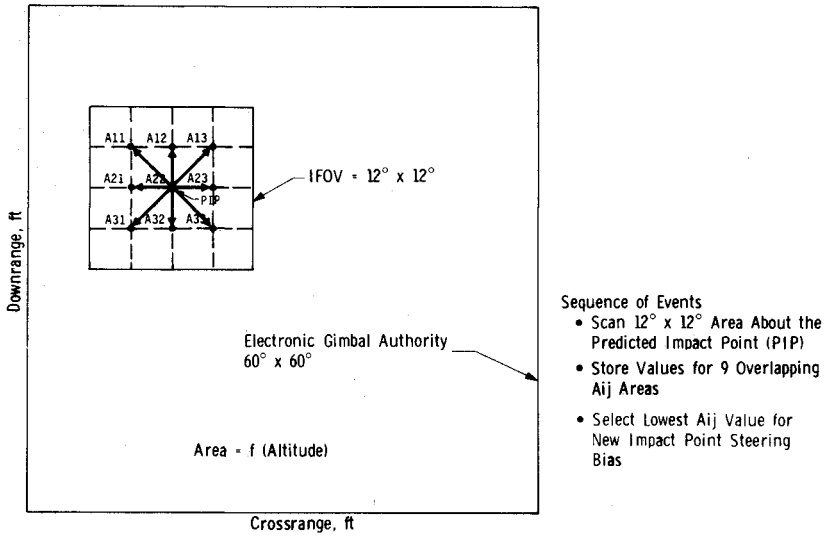

Fig. 4 Scan layout.

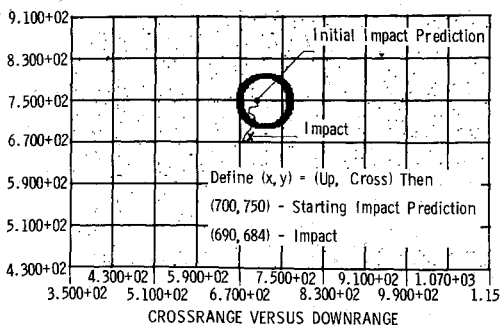

Fig. 5 Random surface plus single crater.

surface, which provides a trace of the changing impact prediction with respect to the surface during the simulated terminal descent and landing.

Impact Prediction

The first function of a PLS[3] is to calculate the PIP. The impact coordinate is calculated by numerically integrating a set of equations (derived from the equations of motion) and by making certain simplifying assumptions for the so-called gravity turn that is executed by the terminal descent guidance and control system. The equations are numerically integrated until the vehicle enters the constant velocity phase, which produces a zero additional downrange distance because of near-vertical descent. In the PLS[3] simulation, the impact prediction was calculated once per second during descent to produce pointing commands for the sensor.

Sensor Model

The sensor model functionally describes the estimate of surface roughness generated by electro-optical scanning. The sensor requires a pointing command from the flight computer, which is calculated using

$$\mathbf{P}_3 = (\mathbf{P}_1 - \mathbf{P}_2)/\|\mathbf{P}_1 - \mathbf{P}_2\|$$

where $\mathbf{P}_1$ = impact prediction, and $\mathbf{P}_2$ = current position. The electro-optical scanning is a function of altitude and the fixed intaneous FOV, which specify the size of the area to be scanned and the resolution. This scanning mechanization identifies the best landing site by selecting the coordinate with the lowest figure of merit. The probability of a safe landing is increased because the closed-loop guidance system constantly steers toward the area with the lowest obstacle density.

Guidance

Only guidance calculations that determine the inputs necessary for the current reference mission guidance and control system to steer toward the desired landing site are required. A bias velocity vector $\mathbf{V}_B = (UBIAS, VBIAS, WBIAS)$ is calculated by

$$\mathbf{V} = (\mathbf{P}_1 - \mathbf{P}_2)/TLP$$

where $\mathbf{P}_1$ = predicted impact, $\mathbf{P}_2$ = desired impact, and TLP = time remaining. The size of the bias velocity vector is then limited to ensure stability of the landing vehicle and was verified by a simulated landing where a landing coordinate was chosen once per second based on a random number. This so-called random walk to the surface represented a worst-case demand on the system, and the lander remained stable resulting in a successful landing.

System Integration

The general flow of the PLS[3] is shown in Fig. 6. The position and velocity vectors available from the flight computer were used to calculate the PIP and to issue a pointing command to the camera. After scanning the surface, the camera performs the

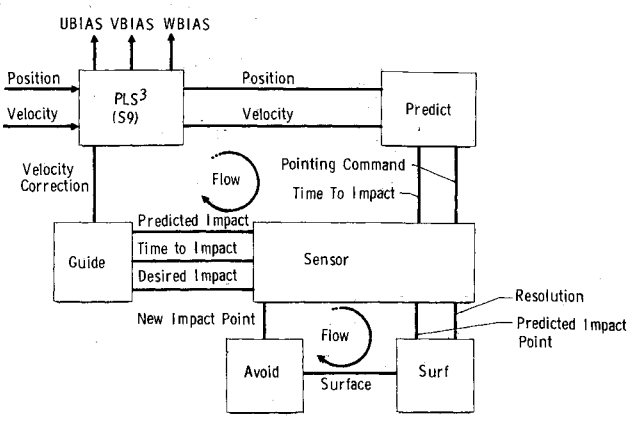

Fig. 6 PLS[3] module flow diagram.

decision logic and reports the best landing site location. Guidance calculations determine the bias velocity vector required by the reference system. The interface required with the reference lander guidance and control system is minimal. The programs were coded and run on a CDC 6500 computer. The fuel cost to maneuver up to 240 ft was a maximum of 2 additional pounds of fuel with respect to the nominal fuel requirement of 106.3 lb.

Breadboard Testing

The PLS[3] was breadboarded to demonstrate the feasibility of generating estimates of surface roughness by electro-optical scanning. The critical consideration was the capability of the PLS[3] to avoid surface obstacles. Several different surfaces were generated to test the system.

The approach was to scan a simulated planetary surface in a particular pattern to arrive at a measure of surface roughness, thereby providing the data required to select a desirable landing site. Changes in altitude were simulated by using a zoom lens. The camera beam was electronically aimed at the sequential areas to be scanned. The video signal was filtered, modulated, integrated, and displayed on an electronic counter and scope. The count was a direct measure of surface contrast in three sequential frequency bands. Nine areas were scanned about the center point, and six figures of merit (two for each frequency band) were generated for each of the nine areas. After analyzing these data and selecting the area with the lowest count (minimum contrast), the camera was refocused on a smaller area with the centre point coinciding with the center of the lowest count area selected from the previous scan. This was done to simulate varying altitudes.

Breadboard System Description

The target or surface to be observed consisted of a transparency of the selected photograph, which was illuminated by a dc fluorescent light source. A 25- to 100-mm zoom lens was mounted on a $1\frac{1}{2}$-in. image dissector tube that was used to observe the surfaces. The camera had a 300-line scan with a 0.0035 aperture. A 2-in.^{2} sector was scanned with the zoom lens set at $f5.6$ with a focal length of 25 mm. The scan rate was 30 lines per frame with 30 elements (pictels) per line, which provided 900 pictels per frame per second. A single-line scan mode was used to evaluate frequency content, position the scan sector, and set the thresholds for the three frequency bands. The full band video signal was then passed through a frequency-limiting filter to separate the surface feature characteristics. The reflectances from the various features (craters, slopes, ridges, breaks, boulders, rocks, etc) indicate that each frequency band provides a measure of a peculiar set of surface characteristics. The outputs from the three frequency-limiting channels were in analog form and represented the size, extent, and reflectance characteristics of the surface features. The three preselected frequency bands used in this experiment were 20–160 Hz for the

low-frequency band, 80–320 Hz for the midfrequency band, and 320–1000 Hz for the high-frequency band.

After filtering, the video signal was passed through a threshold detector and a pulse generator that generated a pulse as the signal level exceeded the preselected threshold and terminated the pulse as the signal decayed below this threshold. This signal triggered a 2-kHz pulse generator to detect large areas of contrast. This high-frequency modulation is necessary because the unmodulated signal would be counted as a single point of contrast with no consideration given to the pulse width (i.e., large obstacles or slopes). The digital counter counts the pulses, which are a direct measure of surface roughness. The count is displayed on an electronic counter for each bandwidth.

Experimental Results

A typical experiment consisted of scanning a boulder field at medium altitude, followed by a low-altitude scan, centered on the area with the best figure of merit as determined by the scan at medium altitude. A photograph of the lunar surface containing a dense distribution of rocks and boulders was selected to provide maximum strain on the breadboard system's ability to locate a relatively smooth area. The camera was electronically aimed so the instantaneous 12° FOV was approximately centered on the photograph (Fig. 7). Again, each figure of merit was determined by scanning a 2 × 2 in. area.

The larger area scanned contains the figures of merit obtained using the modulated midfrequency signal. A desirable landing area is not obvious from the photograph because of the high density of rocks and boulders. Closer visual examination of the scanned surface areas verifies that the middle and lower-middle areas contain a lower density of rocks and boulders, as indicated by the respective figures of merit. The lower-middle area was identified by the breadboard system as the best area by all frequency bands. The camera's instantaneous FOV was then aimed electronically at the center of the lower-middle area and the zoom lens adjusted to reduce the size of the area to be scanned to 1 × 1 in., thus simulating a decreased altitude. The area scanned is outlined by the smaller squares, which also contain figures of merit generated by the midfrequency band signal. The reduced size of the area of scan introduces the influence of smaller rocks on the figures of merit, and increases the relative influence of the rocks and boulders picked up by the scan at the higher altitude. The best landing site identified by the midfrequency signal can be visually verified by noting a relatively smaller density of obstacles in this region. The dynamic response of the system, which would produce another steering decision from a reduced FOV, would isolate the obstacles identified in the low-frequency channel and would avoid them as long as a smooth area is indicated.

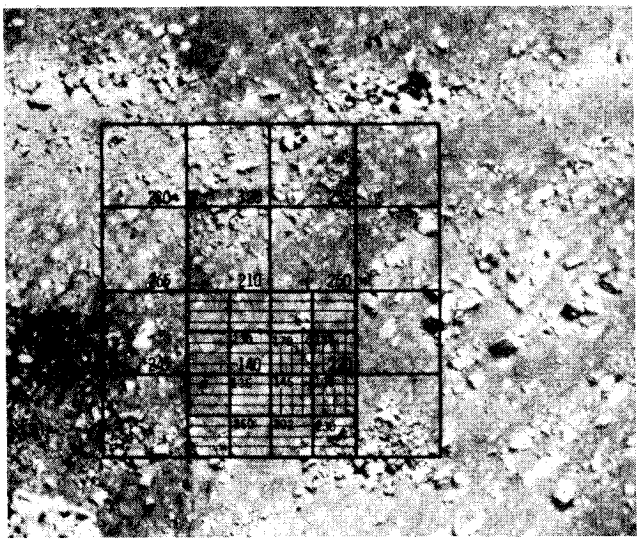

Fig. 7 Simulated site selection.

Conclusions

The feasibility of a PLS[3] has been established. State-of-the-art miniature hardware available for the Viking mission could result in a very lightweight, sterilizable system. For every surface generated in the simulations, the lander found a smooth area and executed a successful landing. Analysis of the results indicates that a PLS[3] requiring minimal interface with the lander, negligible additional fuel, and minimal additional flight computer software can be built. In every case, the breadboard system identified a desirable landing area. The important conclusion from breadboard testing is that the desired surface information is present in the raw camera signal and can be extracted. It is concluded that a PLS[3] could provide greater mission flexibility and could be adapted to future missions with a minimum effect on the present Viking lander configuration.

Detection of Flight Vehicle Transition from Base Measurements

BRUCE M. BULMER*
Sandia Laboratories, Albuquerque, N. Mex.

Introduction

THE prediction of boundary-layer transition on full-scale conical re-entry vehicles (RV's) in ballistic flight is a necessary and important part of preflight design analyses. Empirical prediction techniques inherently must rely upon flight transition data obtained from vehicles having similar configurations and heatshield ablation characteristics. While it is usually advantageous to have complete instrumentation onboard a vehicle to detect the onset of transition, most RV's use ablative heatshields for high-performance flight. As a result, complete heatshield instrumentation (particularly for RV frustum surface temperature, which is probably the best indication of transition) is often impractical and in some instances impossible.

In contrast, base data measurements are generally very easy to obtain because the thermal environment in the base-flow region is far less severe than on the frustum preceding the base. Therefore, instrumentation problems associated with the extreme thermal environment on the frustum are almost entirely eliminated on the base. Base pressure and heat-transfer measurements provide extremely useful sources of transition data because the characteristics of base flow are highly dependent upon the upstream boundary-layer condition on the frustum immediately preceding the base (for examples, see Cassanto, Rasmussen, and Coats[1]). As a result, changes in the upstream boundary-layer condition that result from transition onset are immediately detected by the base instrumentation. This Note presents base pressure and heat-transfer data from two RV flight tests that provide very distinct indications of transition onset. These transition indicators are compared with several other indicators for each flight.

Received September 13, 1972; revision received November 27, 1972. This work was supported by the U.S. Atomic Energy Commission.

Index categories: Re-Entry Vehicle Testing; Boundary-Layer Stability and Transition; Jets, Wakes, and Viscid-Inviscid Flow Interactions.

* Member, Technical Staff, Re-Entry Vehicle Aerothermodynamics Division. Member AIAA.